

Research Article

Multivariate Interpolation of Precipitation Using Regularized Spline with Tension

Jaroslav Hofierka
*Department of Geography and
Geoecology
University of Presov*

Juraj Parajka
*Experimental Hydrological Station
Institute of Hydrology
Slovak Academy of Sciences*

Helena Mitasova
*Department of Marine, Earth and
Atmospheric Sciences
North Carolina State University*

Lubos Mitas
*Department of Physics
North Carolina State University*

Abstract

Regularized Spline with Tension (RST) is an accurate, flexible and efficient method for multivariate interpolation of scattered data. This study evaluates its capabilities to interpolate daily and annual mean precipitation in regions with complex terrain. Tension, smoothing and anisotropy parameters are optimized using the cross-validation technique. In addition, smoothing and rescaling of the third variable (elevation) is used to minimize the predictive error. The approach is applied to data sets from Switzerland and Slovakia and interpolation accuracy is compared to the results obtained by several other methods, expert-drawn maps and measured runoff. The results demonstrate that RST performs as well or better than the methods tested in the literature. The incorporation of terrain improves the spatial model of precipitation in terms of its predictive error, spatial pattern and water balance.

1 Introduction

Spatially distributed measurements of precipitation have gained renewed interest in connection with climate-change impact studies, determination of water budgets at different temporal and spatial scales, as well as validation of atmospheric and hydrologic models. Precipitation values are usually available from a limited number of meteorological stations and spatial estimates of precipitation fields are obtained by interpolation

Address for correspondence: Lubos Mitas, Department of Physics, North Carolina State University, Box 8202, Raleigh NC 27695-8202, USA. E-mail: limitas@unity.ncsu.edu

techniques. Mountainous environments pose a special challenge to spatial interpolation because the measured data are sparse, often restricted to lower elevations while spatial variability in precipitation can be substantial. Various approaches were therefore developed to improve the interpolation results by incorporation of the impact of topography, for example, MTCLIM (Running et al. 1987, Thornton et al. 1997), PRISM (Daly et al. 1994), ANUSPLIN (Hutchinson and Bischof 1983, Hutchinson 1995).

Tabios and Salas (1985) evaluated several techniques for interpolation of precipitation and concluded that geostatistical methods were superior to Thiessen polygon, polynomial interpolation and inverse-distance weighting methods. Custer et al. (1996) compared ANUSPLIN (Hutchinson 1995) with an expert-drawn precipitation map for Montana and found that both maps were similar, with over 50% cells identical; however, the two maps differed in areas of the lowest and the highest elevation and the ANUSPLIN-generated map had richer spatial pattern, due to the selection of a relatively high digital elevation model (DEM) resolution. The Spatial Interpolation Comparison 97 (SIC 97, Dubois 1998) compared the results of interpolation of daily precipitation data for Switzerland obtained by more than 20 different methods, including Inverse Distance Weighting, Kriging, Radial Basis Functions (Multiquadrics and Splines), Neural Networks, Fuzzy Logic Interpolators and others (Dubois 1998). The estimates with the lowest RMSE were obtained by multiquadric functions with anisotropy and the study has demonstrated that performing a geostatistical analysis of data is helpful for selecting an appropriate interpolation method and its parameters. Incorporation of topography in this study did not lead to improved results for the tested methods. Parajka (1999) compared kriging and co-kriging methods with respect to an expert-drawn precipitation map. The cross-validation analysis in this study has shown that kriging estimates provided reasonable results in regions with sufficiently dense observations, but in mountainous regions with sparse data it did not reflect the impact of topographical patterns. The co-kriging method, which included the effect of topography, provided more accurate and realistic estimates.

One of the spline interpolation functions, which has not been included in the previous studies, but which has performed very well in other applications is the Regularized Spline with Tension (RST) (see Mitasova and Mitas 1993, McCauley and Engel 1995, Rohling et al. 1998 for examples). Its application to interpolation of precipitation with incorporation of topography was demonstrated for a sample data set from South America (Mitasova et al. 1995), indicating that this method can be a suitable choice for effective interpolation of precipitation in a region with significant variability in terrain. The method is relatively simple to use, does not require regionalization of data and its implementation in GRASS5 (GRASS 2002) makes its use efficient for GIS applications. Because it does not depend on prior climatologically extracted covariances it can better adapt to seasonal changes in windward/leeward slopes as well as to the occurrence of both positive and negative relationships between precipitation and elevation in the study area.

Our study aims to advance the development of methodology for interpolation of precipitation in mountainous regions within a general GIS, based on multivariate RST with optimized parameters. We investigate the impact of parameters and incorporation of the third variable (elevation) on the predictive error of interpolation and compare the results for daily and annual mean precipitation with other methods, an expert drawn map and measured runoff. Based on the results of comprehensive testing, we suggest an effective strategy for this type of application.

2 Multivariate Interpolation by Regularized Spline with Tension

The RST method has been described by Mitasova and Mitas (1993) (an earlier version called Completely Regularized Spline) and Mitasova et al. (1995) (the general d -dimensional formulation with applications for 2D, 3D, and 4D data). We briefly recall the basic principles of the method and then focus on issues of selection of parameters important for interpolation of precipitation data.

2.1 Basic Principles and Radial Basis Functions

In general, a spline function $S(\mathbf{x})$ fulfills the condition of minimizing the deviation from the measured points and at the same time its smoothness seminorm $I(S)$ (e.g. Wahba 1990):

$$\sum_{j=1}^N |p^{[j]} - S(\mathbf{x}^{[j]})|^2 w_j + w_0 I(S) = \text{minimum} \tag{1}$$

where $p^{[j]}$ are the values measured at discrete points $\mathbf{x}^{[j]} = (x_1^{[j]}, x_2^{[j]}, \dots, x_d^{[j]})$, $j = 1, \dots, N$ within a region of a d -dimensional space, w_j, w_0 are positive weighting factors and $I(S)$ is the measure of smoothness (smooth seminorm or roughness penalty). For $w_0/w_j = 0$ the function $S(\mathbf{x})$ passes exactly through the data. The general solution of the minimization problem given by equation (1) can be expressed as a sum of two components (Talmi and Gilat 1977)

$$S(\mathbf{x}) = T(\mathbf{x}) + \sum_{j=1}^N \lambda_j R(\mathbf{x}, \mathbf{x}^{[j]}) \tag{2}$$

where $T(\mathbf{x})$ is a ‘trend’ function and $R(\mathbf{x}, \mathbf{x}^{[j]})$ is a *radial basis function* with an explicit form depending on the choice of the $I(S)$. The smoothness seminorm $I(S)$ for the RST method has been designed to synthesize in a single function properties of several previously known splines, such as the Thin Plate Spline (Duchon 1976), the Thin Plate Spline with Tension (Franke 1985, Mitas and Mitasova 1988), and the Regularized Thin Plate Spline (Mitas and Mitasova 1988). These desired properties include an explicit form, multi-variate formulation, smooth derivatives of higher orders, variational freedom through tension, and anisotropy.

The seminorm that fulfills these requirements includes derivatives of *all orders* with weights rapidly decreasing with the increasing derivative order. For $d = 2$ it has the following form:

$$I^2(S) = \sum_{\alpha} B_{\alpha} \int \int_{\Omega} \left[\frac{\partial^{|\alpha|}}{\partial x_1^{\alpha_1} \partial x_2^{\alpha_2}} S(\mathbf{x}) \right]^2 dx_1 dx_2 \tag{3}$$

where $\alpha = (\alpha_1, \alpha_2)$ is a multiindex ($\alpha_1 = 0, 1, 2, \dots, \alpha_2 = 0, 1, 2, \dots$), with $|\alpha| = \alpha_1 + \alpha_2$ and $\{B_{\alpha}\}$ are nonnegative constants, in our case

$$B_{\alpha} = \begin{cases} 0, & |\alpha| = 0 \\ \frac{|\alpha|!}{\alpha_1! \alpha_2! \varphi^{2|\alpha|} (|\alpha| - 1)!}, & |\alpha| > 0 \end{cases} \tag{4}$$

where φ is a relative reciprocal weight of particular terms in the sum (*generalized tension*) which provides the control over the influence of derivatives of certain order on the resulting function. With this particular choice of coefficients, the RST functions have the following explicit form for $d = 2, 3$ (Mitasova et al. 1995)

$$S(\mathbf{x}) = a_1 + \sum_{j=1}^N \lambda_j \{-[E_1(\rho) + \ln \rho + C_E]\}, \quad d = 2 \tag{5}$$

$$S(\mathbf{x}) = a_1 + \sum_{j=1}^N \lambda_j \left[\sqrt{\frac{\pi}{\rho}} \operatorname{erf}(\sqrt{\rho}) - 2 \right], \quad d = 3 \tag{6}$$

where $\rho = (\varphi r/2)^2$, $r^2 = \sum_{i=1}^d (x_i - x_i^{[j]})^2$ is the squared distance, $C_E = 0.577215..$ is the Euler constant, $E_1(\cdot)$ is the exponential integral function and $\operatorname{erf}(\cdot)$ is the error function (Abramowitz and Stegun 1964). The coefficients $a_1, \{\lambda_j\}$ are obtained by solving the following system of linear equations

$$a_1 + \sum_{j=1}^N \lambda_j [R(\mathbf{x}^{[i]}, \mathbf{x}^{[j]}) + \delta_{ji} w_o/w_j] = z^{[i]}, \quad i = 1, \dots, N \tag{7}$$

$$\sum_{j=1}^N \lambda_j = 0 \tag{8}$$

where $w = w_o/w_j$ is the smoothing parameter. Computational demands due to the solution of this system have been cited as a major limitation for application of this type of splines; however, the problem has been satisfactorily resolved by a segmentation procedure implemented in the GRASS version of the RST, *s.surf.rst* (GRASS 2002). This program has been routinely used to interpolate data sets with hundreds of thousands of points (e.g. Gardner et al. 1994, Mitasova et al. 1995, Mitas and Mitasova 1999).

The RST method is related to the bivariate and trivariate spline methods implemented in ANUSPLIN (Hutchinson 1998a, b). It is based on the same general condition given by equation (1); however, ANUSPLIN uses a different smoothness seminorm $I(S)$ leading to a different behavior of the interpolation function.

2.2 Anisotropy

Spatial distribution of precipitation is often driven by wind orientation and topography that may result in an anisotropic spatial pattern. Using the fact, that for the RST function, the change of scale is equivalent to the change in the tension parameter, anisotropy can be implemented by rotating the coordinate system by an angle θ (direction of anisotropy) and then rescaling one axis according to the anisotropy magnitude. For $d = 2$, the transformation from original coordinates $\mathbf{x} = (x_1, x_2)$ to new coordinates $\mathbf{x}' = (x'_1, x'_2)$ is simply

$$x'_1 = x_1 \cos(\theta) + x_2 \sin(\theta) \tag{9}$$

$$x'_2 = -x_1 \sin(\theta) + x_2 \cos(\theta) \tag{10}$$

and the distances are then computed as

$$r^2 = s(x_1 - x_1^{[j]})^2 + (x_2 - x_2^{[j]})^2 \quad (11)$$

where $s = s_1/s_2$ is a scaling coefficient expressed here as a ratio between the scaling in the x_1' and x_2' axis respectively. The rotated and rescaled distances are then used in the solution of equations (7) and (8) as well as for the computation of interpolated values at the grid points. The direction and scaling of the anisotropy can be found using standard geostatistical tools, for example, GSLIB (Deutsch and Journel 1992) or VARIOWIN (Pannatier 1996). The generalization of the coordinate transformation for $d = 3$ is straightforward.

2.3 Interpolation with Influence of Additional Variable

To interpolate precipitation with the influence of topography an approach similar to the one proposed by Hutchinson and Bischof (1983) can be used. Given the N values of precipitation $p^{[j]}$ measured at discrete points, $\mathbf{x}^{[j]} = (x_1^{[j]}, x_2^{[j]}, x_3^{[j]})$, $j = 1, \dots, N$ within a certain region of a 3-dimensional space we compute a function $p = F(x_1, x_2)$ representing the spatial distribution of precipitation over the terrain surface $x_3 = G(x_1, x_2)$ as

$$p = F(x_1, x_2) = S(x_1, x_2, cG(x_1, x_2)) \quad (12)$$

where c is a vertical rescaling parameter, and $S(\cdot)$ is the trivariate RST function. Equation (12) can be interpreted as an intersection of the RST volume model of precipitation with the terrain surface. This approach thus captures a more complex, spatially and temporally variable relation between precipitation and elevation than the traditional methods based on statistical correlation.

2.4 Control parameters

One of the advantages of the RST method is its flexibility within the single radial basis function, as opposed to the often subjective task of selecting a suitable variogram in kriging. To reflect the behavior of modeled phenomenon, the function can be tuned by a set of the following parameters:

- tension φ ,
- smoothing w ,
- anisotropy: rotation and scale (θ, s) ,
- vertical scaling c ,
- resolution and smoothing of DEM.

The tension φ , smoothing w , anisotropy (θ, s) , and vertical scaling c are internal RST parameters and control the character of the resulting surface or volume (Mitas and Mitasova 1999). The resolution and smoothing of the DEM influences the spatial variability of the “intersection” surface $x_3 = G(x_1, x_2)$ and hence the spatial variability of the resulting precipitation map $p = F(x_1, x_2)$. The parameters can be selected empirically, based on the knowledge of the modeled phenomenon, or automatically, by minimization of the predictive error estimated by a cross-validation procedure (Mitasova et al. 1995).

2.5 Evaluation of Accuracy

The predictive accuracy of interpolation methods is often evaluated by the cross-validation procedure. The method is based on removing one data point at a time, performing the interpolation for the location of the removed point using the remaining samples and calculating the residual between the actual value of the removed data point and the estimate for this point obtained from the remaining samples. This procedure is repeated until every sample has been, in turn, removed. The overall performance of the interpolator is then evaluated as the root-mean of squared residuals (Tomczak 1998). Low root-mean-squared error (RMSE) indicates an interpolator that is likely to give more reliable estimates in the areas with no precipitation data. The cross-validation can be used to find optimal interpolation parameters by minimizing the RMSE (Mitasova et al. 1995). However, Hutchinson (1998a) found that the cross-validation does not always represent a reliable estimate of model error, especially when short range correlation in data is present. To evaluate the reliability and consistency of the predictions, it is therefore appropriate to use additional evaluation methods or tools.

Comparison with expert hand-drawn precipitation maps (e.g. Custer et al. 1996, Parajka 1999) and maps of derived hydrological processes can provide some insight into the capabilities of the interpolation method to adequately represent the behavior of modeled phenomenon including the features which may not be directly incorporated in the data. Annual mean precipitation, evapotranspiration, and elementary runoff can be represented by continuous fields. Besides continuity, these phenomena must fulfill balancing constraints (i.e. the hydrologic water balance) and other laws (vertical and horizontal geographical zonality, relationships to other spatial physiographic variables). Sometimes this complexity of interrelations is used as an argument against automated mapping approaches, especially in areas with insufficient density of observations (Gottschalk and Krasovskaia 1998). The manually drawn maps include the expert's local knowledge and experience (Parajka and Szolgay 1998) that may be difficult to obtain from the data themselves, especially if the data are sparse. On the other hand, manual mapping is time consuming, subjective and the expert could use an incorrect 'mental' model (Church et al. 1995).

Because the interpolated precipitation maps are often used as inputs for hydrologic models it is useful to evaluate their cross-consistency with respect to balancing constraints against measured runoff data. The grided runoff maps can be computed within the framework of the hydrologic water balance as:

$$R = P - E \quad (13)$$

where $R[mm/year]$ is runoff, $P[mm/year]$ is interpolated precipitation, and $E[mm/year]$ is interpolated evapotranspiration. Areal averages of runoff derived from grided runoff maps can be compared to runoff values measured in basins. If the impact of error in the evapotranspiration map can be considered negligible (e.g. range of E values is small), then statistical comparison of the differences between observed and computed basin runoff averages can be used for the evaluation of accuracy and spatial cross-consistency of precipitation fields obtained by different methods.

3 Application to Precipitation Data

The RST method was evaluated using two regions with significant variability in elevation. First, we applied the method to the daily precipitation data from Switzerland used for the Spatial Interpolation Comparison (SIC97) (Dubois et al. 1998). This application was useful for comparison of RST with a number of other methods, before devoting our effort to a more detailed study and application to annual mean precipitation for Slovakia.

3.1 Daily Precipitation for Switzerland

A daily precipitation data set from Switzerland was obtained from the SIC'97 data available at ftp://ftp.geog.uwo.ca/SIC97/intro/SIC_Introduction.htm. It consists of 100 rainfall measurements randomly extracted from a data set of 467 measurements made in Switzerland on the 8th of May 1986 (Table 1). The participants of SIC'97 had to estimate the daily rainfall at the 367 remaining locations (Table 1, Plate 2). Along with the precipitation data, a DEM with a horizontal resolution of 1009.975 m (376 columns \times 253 rows) was provided as secondary information, along with country borders to define the study area.

First, we interpolated the precipitation data by 2D RST. The tension and smoothing were optimized by minimizing the cross-validation error (RMSE) using the provided 100 points, resulting in $\varphi = 104$ and $w = 0$. These parameters were used to interpolate the raster maps of precipitation and compute the residuals and RMSE for the withheld 367 points. We found that the parameters based on cross-validation were not optimal and different values of tension and smoothing, $\varphi = 20$ and $w = 0.6$, resulted in the lowest RMSE for the remaining 367 points (Table 2). The RMSE for $\varphi = 104$ and $w = 0$ was 6.74 for the given 100 points and 5.89 for the withheld 367 points, while for $\varphi = 20$ and $w = 0.6$ the RMSE was 7.41 for the given 100 points and 5.48 for the 367 points. It must be noted that all SIC'97 interpolations presented in Table 2 were accomplished without the possibility to optimize the interpolation parameters using the 367 withheld points. Therefore a fair comparison for the 2D RST can be made only for $\varphi = 104$ and $w = 0$.

We also investigated the possibility to improve the predictive accuracy for the 2D RST by incorporating anisotropy, as several authors did in SIC'97 (e.g. Thielen 1998, Tomczak 1998). We found that the anisotropy with $\theta = 60^\circ$ and $s = 0.25$ reduced the

Table 1 Statistics for the 100 given daily rainfall values [mm] and for the 367 withheld values (Dubois 1998).

Number of observations	100	367
Minimum	1.0	0.0
Maximum	58.5	51.7
Mean	18.01	18.53
Variance	136.14	123.58
Standard deviation	11.67	11.2
Skewness	0.96	0.57
Kurtosis	0.47	-0.37

Table 2 The 10 methods with the lowest RMSE from SIC'97 (compiled from Dubois et al. 1998) and the RMSE for the 2D and 3D RST. The 2D RST results with optimum parameters found by minimizing the RMSE for the 367 points are denoted by *. The remainder of the methods used only 100 points to optimize the parameters. While the methods are ordered according to the RMSE, the order does not represent their performance because the RMSE reflects only one aspect of accuracy. For different criteria, e.g. range, the order may be different.

Method	RMSE [mm]
*2D RST with anisotropy $\varphi = 20, w = 0.6, \theta = 60^\circ, s = 0.25$	5.20
Multiquadric with anisotropy (Thiessen 1998)	5.31
3D RST $\varphi = 10, w = 0.1, c = 20, d = 1$ km	5.39
Linear kriging (Saveliev et al. 1998)	5.46
*2D RST $\varphi = 20, w = 0.6$	5.48
Multiquadric (Thiessen 1998)	5.57
2D TPS (untransformed data, Hutchinson 1998a)	5.60
Neural Network Residual Kriging (Demyanov et al. 1998)	5.63
Probability Class Kriging (Allard 1998)	5.74
IRF-K (Bruno and Capicotto 1998)	5.74
2D RST $\varphi = 104, w = 0.0$	5.89
Ordinary kriging with anisotropy (Atkinson and Lloyd 1998)	5.97
Indicator kriging with anisotropy (Atkinson and Lloyd 1998)	6.00
Zone kriging with anisotropy (Saveliev et al. 1998)	6.14

RMSE to 5.2 mm (Table 2, Plate 2a) that is the smallest RMSE among the compared interpolation methods.

Despite the fact that several authors from SIC'97 have shown lack of correlation between elevation and precipitation (e.g. Allard 1998, Atkinson and Lloyd 1998) and tri- and quint-variate partial thin plate splines of Hutchinson (1998b) performed worse than the bivariate case, we have interpolated the data by the 3D RST without anisotropy to evaluate its capabilities to capture the impact of terrain on precipitation. The parameters were again optimized by minimizing the cross-validation error using the provided 100 points, resulting in $\varphi = 10, w = 0.1$ (Table 2), which also resulted in the lowest RMSE for the remaining 367 points. Therefore, for the 3D case, the parameters found by cross-validation using only the given 100 points were considered optimal. The RMSE was lower than for the isotropic 2D RST and slightly higher than for the anisotropic 2D RST (Table 2). Incorporation of terrain in 3D RST at 1km resolution has substantially increased the complexity of the spatial pattern of precipitation when compared with the 2D RST map (Plate 2a,b, see plate section). This complexity can be reduced by using a smaller value of vertical rescaling c , or by using a DEM with lower resolution (Thornton et al. 1997). However, while leading to smoother, less complex precipitation maps, these approaches increased the RMSE. The comparison with the 2D RST interpolation from all 467 points (Plate 2c) shows that using only the given 100 points without the elevation leads to simplification of the precipitation pattern (Plate 2a); however, the pattern improves when the same 100 points are used together with elevation (Plate 2b). Moreover, the introduction of

elevation captured both positive and negative relationships between precipitation and elevation in different subregions of the study area. It is reasonable to expect that incorporation of anisotropy into 3D RST may provide an even better result and it is therefore being considered for implementation.

3.2 Annual Mean Precipitation for Slovakia

Long-term annual mean precipitation values were obtained from 423 meteorological stations and from 12 storage gauges of the Slovak Hydrometeorological Institute network. Length of records was 30 years (1951–80) for all meteorological stations and for four storage gauges, and 20 years (1961–80) for eight storage gauges. General statistics of observed precipitation values are presented in Table 3. The elevation data were provided with 1 km resolution (Figure 1). Manually produced isoline maps of the annual mean precipitation and evapotranspiration from the 1951–80 long-term period, as well as long-term (1951–80) annual mean runoff data from 57 gauged sites were used for the evaluation of the interpolation methods. The gauged sites represent outlets of basins ranging in size from 40 to 3800 km² (Figure 1).

We have tested the suitability of both 2D and 3D RST for interpolation of this long-term precipitation data. First, the impact of change in various parameters on the predictive accuracy of 3D RST was evaluated using the cross-validation procedure for all 435 data points from Slovakia (Figure 2) with the following results:

- RMSE sharply increases for lower values of tension if smoothing $w = 0$. A small value of smoothing (e.g. $w = 0.1$) improves the behavior of the function (Mitasova et al. 1995, Rohling et al. 1998) and results in the lowest RMSE values with the optimal value of the tension $\varphi = 15$. Higher values of smoothing increase the RMSE (Figure 2).
- Higher vertical scaling c lowers the impact of changing the tension parameter, with $c = 50$ leading to the lowest RMSE.
- The resolution and smoothing of the third variable (DEM) also have an impact on the RMSE (Thornton et al. 1997). For the optimized values of smoothing, tension and vertical scaling, DEM resolutions 500, 1000 and 2000 m resulted in 73.2, 72.3 and 80.3 mm RMSE, respectively. We have also smoothed the DEM, using the RST program modified for raster data input, with the lowest RMSE achieved for smoothing $w_{el} = 15$. However, when the hydrologic water balance was considered, the best results were obtained for $w_{el} = 5$.

Table 3 Statistics of the 435 observed annual mean precipitation values [mm] in Slovakia

Number of observations	435
Minimum	492
Maximum	2091
Mean	735
Variance	36937.05
Standard deviation	192.19
Skewness	2.416
Kurtosis	9.112

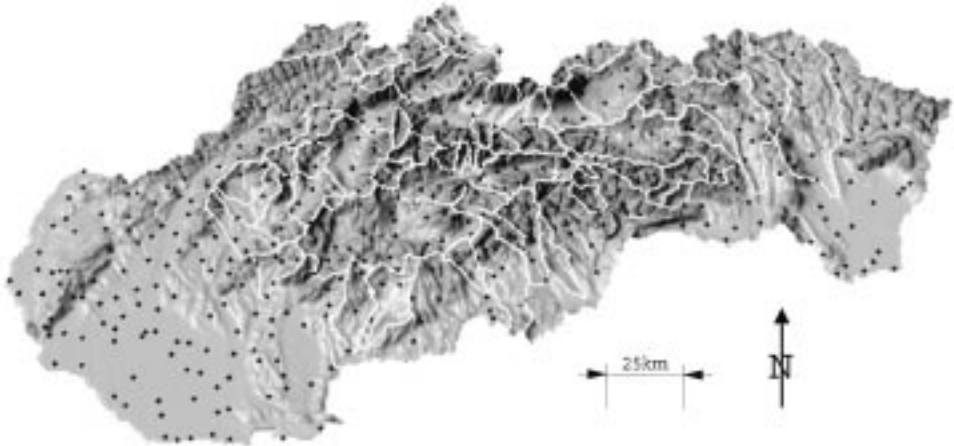


Figure 1 Digital elevation model of Slovakia with precipitation stations and basin boundaries

The tension and smoothing parameters for the 2D RST were optimized using the same approach. The parameters with the minimal RMSE for both 2D and 3D RST are listed in Table 4, and the corresponding precipitation maps are presented in Plate 3, see plate section. The 3D RST map shows patterns that are clearly related to topography, with minimum precipitation at lowlands and increasing precipitation values in the mountains. The most important differences between the 2D and 3D RST maps are in mountainous areas with sparse data. The 3D RST was able to predict high precipitation in these areas that is in agreement with well-known precipitation behavior and observed data from other mountainous areas.

To evaluate the accuracy and validity of precipitation maps interpolated by RST, we compared the results with:

- kriging and co-kriging,
- an expert hand-drawn precipitation map,
- runoff estimates from manual maps, and
- observed runoff.

Table 4 The list of optimal RST parameters for the annual mean precipitation in Slovakia

Parameter	2D	3D
Tension φ	85	15
Smoothing w	0.1	0.1
Vertical scaling c	–	50
Anisotropy	–	–
Smoothing of 3rd variable	–	5.0
Spatial resolution of DEM	–	1000 m
RMSE	93.2 mm	72.3 mm

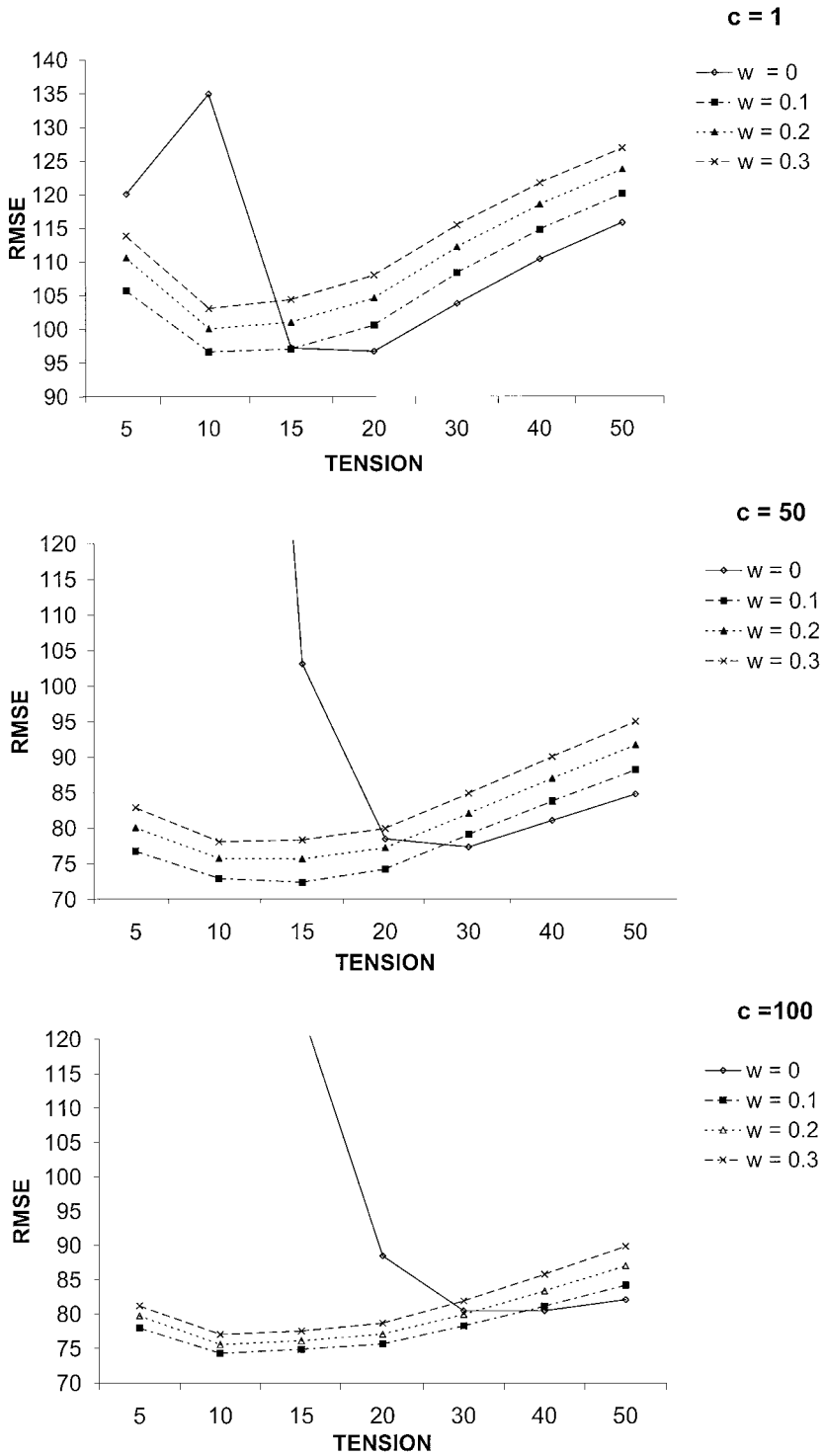


Figure 2 Impact of tension, smoothing and vertical scaling on predictive error for 3D RST

Table 5 Statistical summary of interpolation errors (withheld sample minus interpolated value [mm]) for cross-validation procedure.

	KRIGING	COKRIGING	2D RST	3D RST
count	435	435	435	435
minimum	-213	-319	-694	-417
maximum	701	638	294	765
range	914	957	988	1182
mean	3.10	2.18	1.73	-2.10
std. deviation	92.69	82.29	93.26	72.38
std. error	4.44	3.95	4.47	3.47
sample variance	8592	6772	8697	5239
RMSE	92.6	82.2	93.2	72.3

Results of the comparison between RST, kriging and co-kriging (from Parajka 1999) are presented in Table 5. The most noticeable differences among the interpolation methods are statistical parameters of range and sample variance. Although the 3D RST estimates produced the highest range of differences, the lowest sample variance statistics indicate that this method gives the most satisfactory results. While incorporation of terrain has not reduced the range of errors, it has reduced the sample variance for both co-kriging and the 3D RST.

The spatial cross-consistency of the interpolated precipitation map was evaluated using a comparison with an expert hand-drawn precipitation map (Plate 4a). The map was digitized and transformed to a grid using linear triangulation. A similar approach was used by Parajka (1999), for the evaluation of the cross-consistency between kriging, co-kriging and expert-drawn precipitation maps and by Custer et al. (1996) in their evaluation of ANUSPLIN. The difference between the computed 3D RST map and the digital interpretation of the expert-drawn precipitation map was expressed as a grid map of absolute percentile differences (Plate 4b) and frequencies of each category of difference were tabulated (Table 6). Table 6 shows that the 3D RST precipitation map is closer to the expert-drawn precipitation map than the kriging or the co-kriging estimates. The differences between the 3D RST grid map and the expert-drawn precipitation map are within the range of $\pm 10\%$ for 89% of Slovakia. The largest differences are observed in some mountainous regions with very sparse observations,

Table 6 Absolute percentile differences between grid precipitation maps constructed using 3D RST, 2D RST, kriging and co-kriging methods (PRECIPMAP) and digital interpretation of expert-drawn precipitation map (PMAP).

Area [%] of Slovakia	Absolute % difference $((\text{PRECIPMAP}-\text{PMAP})/\text{PMAP})\times 100$			
	0%–10%	10%–20%	20%–30%	30% and more
3D RST	89%	9%	2%	0%
2D RST	81%	12%	5%	2%
KRIGING	76%	16%	5%	3%
COKRIGING	81%	16%	3%	1%

Table 7 Statistical evaluation of differences between annual runoff basin averages [mm] computed from water balance equation using different precipitation maps and measured runoff values

	PMAP	Kriging	Cokriging	2D RST	3D RST
Mean	23	-67	-13	-53	-7
Standard Error	10.46	12.58	10.06	12.04	8.86
Standard Deviation	78.94	94.98	75.97	90.88	66.93
Sample Variance	6231.81	9021.30	5771.43	8260.02	4479.2
Range	483	421	400	498	324
Minimum	-216	-356	-298	-370	-229
Maximum	267	64	102	128	95
Count	57	57	57	57	57

but in these areas, both the interpolated and hand drawn map have a high level of uncertainty.

The consistency of the results has also been tested within the framework of the hydrologic water balance. For each precipitation map: expert-drawn, 2D RST, 3D RST, kriging, and co-kriging, a long-term annual mean runoff map was created, using a water balance equation (13), with the spatial distribution of evapotranspiration represented by the digital interpretation of an expert-drawn evapotranspiration map. The differences between computed basin averages of annual mean runoff and gaged runoff values for 57 basins were calculated and a statistical comparison of these differences is provided in Table 7. The smallest range, as well as the lowest standard error and sample variance values of the average basin runoff differences indicate, that average basin runoff values computed from 3D RST estimates come the closest to the measured values. In comparison with the other precipitation maps used in this comparison, the 3D RST map performs the best in terms of balancing the constraints of the water balance equation. Table 7 demonstrates that incorporation of terrain into interpolation improves the derived estimates of runoff. Detailed water balance comparison in regions with the highest differences between the expert-drawn precipitation map and 3D RST (Table 8) has shown that the estimates provided by the 3D RST are more accurate with respect to measured runoff than the estimates from the expert-drawn precipitation map. The statistical evaluation presented in Tables 7 and 8 also shows that the range of differences between the annual runoff basin averages computed from different precipitation maps is higher than the range of evapotranspiration for the entire Slovakia, which is about 250 mm. Therefore, the evapotranspiration map error has a negligible impact on the evaluation of different interpolation methods used to compute the precipitation maps.

The results of this comprehensive evaluation using the cross-validation, comparison with kriging, co-kriging, expert-drawn map and runoff demonstrate that the 3D RST method offers reliable and reasonably accurate estimates of annual mean precipitation. Thus, the RST can be used to replace the less efficient manual maps describing the spatial variability of the long-term precipitation over the territory of Slovakia.

Table 8 Statistical summary of differences between computed and measured annual runoff values [mm], for eight basins located in regions with the highest difference between digital interpretation of expert-drawn precipitation map (PMAP) and 3D RST

	PMAP	3D RST
Mean	62	40
Std. Error	48.53	19.26
Std. Deviation	137.26	54.48
Sample Variance	18839	2968
Range	478	129
Minimum	-211	-35
Maximum	267	94
Count	8	8

4 Conclusions

Our study has demonstrated that RST is an appropriate method for interpolation of both daily and long term, annual mean precipitation data. Its accuracy was tested using various criteria and compared to several methods using precipitation data sets for the mountainous countries of Slovakia and Switzerland. It was demonstrated that RST is highly competitive with multiquadrics and kriging approaches. Its accuracy depends on the adequate choice of parameters, especially tension, smoothing and for the 3D RST also the resolution and smoothing of the DEM. The RST parameters can be optimized using cross-validation, however, the procedure does not guarantee optimal parameters for all cases. The criteria for a representative cross-validation data set that would lead to optimal parameters should be further investigated. The incorporation of the third variable – terrain elevation – showed a marked improvement in terms of both interpolation accuracy and the validity of spatial pattern in mountainous areas with sparse data, especially for the long-term precipitation averages.

Interpolation of daily precipitation data was more demanding and sensitive to the density and spatial distribution of data. In situations when daily data depend more on the synoptic situation than on elevation, the RST with anisotropy may be the most appropriate solution (e.g. rainfall under prevailing wind direction). The formulation of RST is suitable for applications requiring interpolation for multiple time periods (e.g. days, hours) using data measured at the same locations. In such a case most of the computation can be done only once and both the reparametrization and computation of the resulting grid is relatively fast. It can be concluded that the RST is a flexible and effective method for spatial interpolation of precipitation data. The incorporation of RST within GRASS5 as *s.surf.rst* and *s.vol.rst* commands makes it especially suitable for GIS applications.

Acknowledgements

We would like to thank the Slovak Hydrometeorological Institute in Bratislava for providing the precipitation data for Slovakia and Dr Pavol Faško for his expert-drawn

precipitation map used in this study. We also appreciate the comments of the anonymous reviewers that helped to improve the paper and provided stimulating ideas for future research.

References

- Abramowitz M and Stegun I A 1964 *Handbook of Mathematical Functions*. New York, Dover
- Allard D 1998 Geostatistical classification and class kriging. *Journal of Geographic Information and Decision Analysis* 2: 87–101
- Atkinson P M and Lloyd C D 1998 Mapping precipitation in Switzerland with ordinary and indicator kriging. *Journal of Geographic Information and Decision Analysis* 2: 72–86
- Bruno R and Capicotto B M 1998 Geostatistical analysis of pluviometric data: IRF-K approach. *Journal of Geographic Information and Decision Analysis* 2: 137–51
- Church M R, Bishop G D and Cassell D L 1995 Maps of regional evapotranspiration and runoff/precipitation ratios in the northeast United States. *Journal of Hydrology* 168: 283–98
- Custer G S, Farnes P, Wilson J P and Snyder R D 1996 A comparison of hand- and spline-drawn precipitation maps for mountainous Montana. *Water Resources Bulletin* 32: 393–405
- Daly C, Neilson R P and Phillips J 1994 A statistical topographic model for mapping climatological precipitation over mountainous terrain. *Journal of Applied Meteorology* 33: 140–58
- Demyanov V, Kanevski M, Chernov S, Savelieva E and Timonin V 1998 Neural network residual kriging application for climatic data. *Journal of Geographic Information and Decision Analysis* 2: 234–58
- Deutsch C V and Journel A G 1992 *GSLIB: Geostatistical Software Library and User's Guide*. New York, Oxford University Press
- Dubois G 1998 Spatial Interpolation Comparison 97: Foreword and Introduction. *Journal of Geographic Information and Decision Analysis* 2: 1–10
- Duchon J 1976 Interpolation des fonctions de deux variables suivant le principe de la flexion des plaques minces. *RAIRO Analysis Numerique* 10: 5–12
- Franke R 1985 Thin plate spline with tension. *Computer Aided Geometrical Design* 2: 87–95
- Gardner R H, Hargrove W W, Levine D A, Pearson S M and Rose K A 1994 Spatial Analysis of Cesium in Sediments of Watts Bar Reservoir. WWW document, <http://research.esd.ornl.gov/CRERP/WATTSBAR/INDEX.HTM>
- Gottschalk L and Krasovskaia I 1998 *Grid Estimation of Runoff Data*. Geneva, World Meteorological Organization Technical Report No 870
- GRASS 2002 Geographic Resources Analysis Support System. WWW document, <http://grass.itc.it>
- Hutchinson M F 1995 Interpolating mean rainfall using thin plate smoothing splines. *International Journal of Geographical Information Systems* 9: 385–403
- Hutchinson M F 1998a Interpolation of rainfall data with thin plate smoothing splines: I, Two dimensional smoothing of data with short range correlation. *Journal of Geographic Information and Decision Analysis* 2: 152–67
- Hutchinson M F 1998b Interpolation of rainfall data with thin plate smoothing splines: II, Analysis of topographic dependence. *Journal of Geographic Information and Decision Analysis* 2: 168–85
- Hutchinson M F and Bischof R J 1983 A new method for estimating the spatial distribution of mean seasonal and annual rainfall applied to the Hunter Valley, New South Wales. *Australian Meteorological Magazine* 31: 179–84
- McCauley J D 1995 Smooth Function Approximation for Surface Representation of Soil Sensor Data. Unpublished PhD Dissertation, Department of Agricultural Engineering, Purdue University
- Mitas L and Mitasova H 1988 General variational approach to the interpolation problem. *Computers and Mathematics with Applications* 16: 983–92
- Mitas L and Mitasova H 1999 Spatial Interpolation. In Longley P A, Goodchild M F, Maguire D J and Rhind D W (eds) *Geographical Information Systems: Principles, Techniques,*

- Management and Applications*. New York, Wiley: 481–92
- Mitasova H and Mitas L 1993 Interpolation by regularized spline with tension: I, Theory and implementation. *Mathematical Geology* 25: 641–55
- Mitasova, H, Mitas L, Brown B M, Gerdes D P, Kosinovsky I 1995 Modeling spatially and temporally distributed phenomena: New methods and tools for GRASS GIS. *International Journal of Geographical Information Systems* 9: 433–6
- Pannatier Y 1996 *VARIOWIN: Software for Spatial Data Analysis in 2D*. New York, Springer
- Parajka J 1999 Mapping long-term mean annual precipitation in Slovakia using geostatistical procedures. In Vlasak P, Filip P and Chara Z (ed.) *Proceedings of the International Conference on Problems in Fluid Mechanics and Hydrology*. Prague, Institute of Hydrodynamics, Academy of Sciences, Czech Republic: 424–30
- Parajka J and Szolgay J 1998 Grid based mapping of long-term mean annual potential and actual evapotranspiration in Slovakia. In Kovar K (ed.) *Hydrology, Water Resources and Ecology in Headwaters*. Wallingford, International Association for Hydrological Sciences Publication No 248: 123–9
- Rohling R N, Gee A H and Berman L 1998 Radial basis function interpolation for 3D ultrasound. Cambridge, UK, Cambridge University Engineering Department, Technical Report No CUED/F-INFENG/TR 327
- Running S W, Nemani R and Hungerford R D 1987 Extrapolation of synoptic meteorological data in mountainous terrain and its use for simulating forest evapotranspiration and photosynthesis. *Canadian Journal of Forestry Research* 17: 472–83
- Saveliev A A, Mucharamova S S and Piliugin G A 1998 Modeling of the daily rainfall values using surface under tension and kriging. *Journal of Geographic Information and Decision Analysis* 2: 62–71
- Tabios G Q and Salas J D 1985 A comparative analysis of techniques for spatial interpolation of precipitation. *Water Resources Bulletin* 21: 365–80
- Talmi A and Gilat G 1977 Method for smooth approximation of data. *Journal of Computational Physics* 23: 93–123
- Thieken A H 1998 Estimating daily regional rainfall fields by multiquadric functions: Accuracy of interpolation and decision making. *Journal of Geographic Information and Decision Analysis* 2: 186–99
- Thornton P E, Running S W and White M A 1997 Generating surfaces of daily meteorological variables over large regions of complex terrain. *Journal of Hydrology* 190: 214–51
- Tomczak M 1998 Spatial interpolation and its uncertainty using automated anisotropic inverse distance weighting (IDW): Cross-validation/jackknife approach. *Journal of Geographic Information and Decision Analysis* 2: 18–33
- Wahba G 1990 Spline models for observational data. In *CBMS-NSF Regional Conference Series in Applied Mathematics, Volume 59*. Philadelphia, PA, Society for Industrial and Applied Mathematics: 1–168

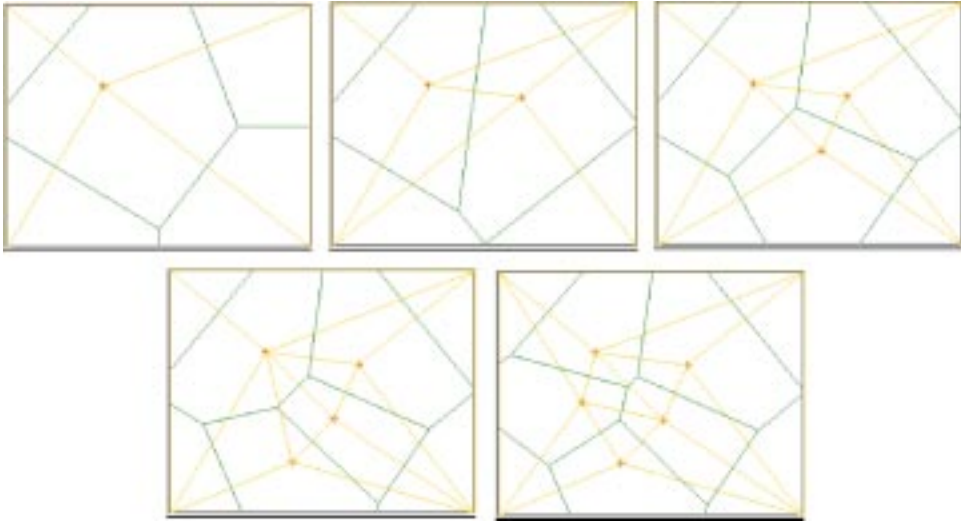


Plate 1 Dynamic insertion into an ordinary Voronoi diagram. Each frame shows the resulting Delaunay triangulation (lighter triangles) and Voronoi tessellation (darker polygons) of progressively adding a new data point. Note that each of the four corners also supply a point

Plate 1 from I Lee and M Gahegan 'Interactive Analysis Using Voronoi Diagrams: Algorithms to Support Dynamic Update from a Generic Triangle-based Data Structure', pages 89–114

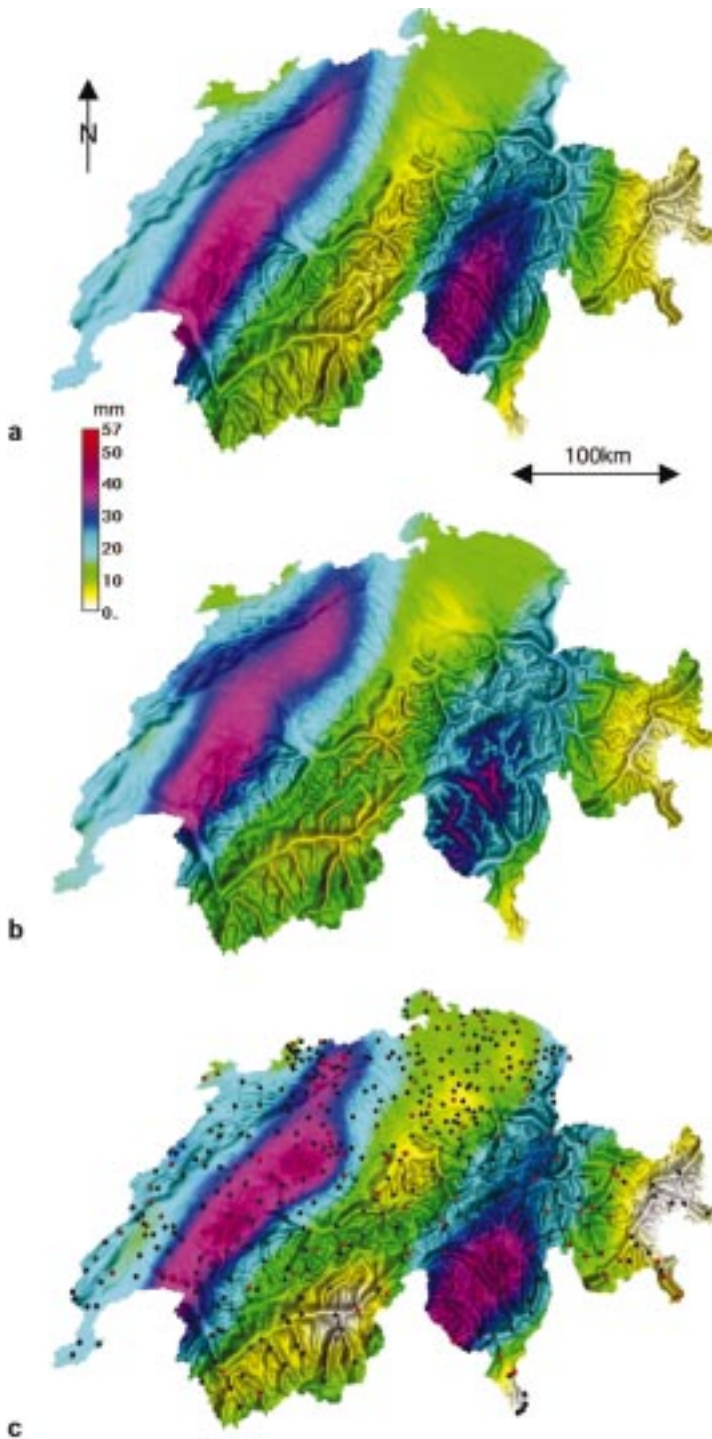


Plate 2 Map of daily precipitation interpolated by a) 2D RST with anisotropy using 100 points, b) 3D RST using 100 points, c) 2D RST using all 467 points, red symbols represent the given 100 points while the black symbols are the sites with the withheld values

Plate 2 from J Hofierka, J Parajka, H Mitasova and L Mitas 'Multivariate Interpolation of Precipitation Using Regularized Spline with Tension', pages 135–150

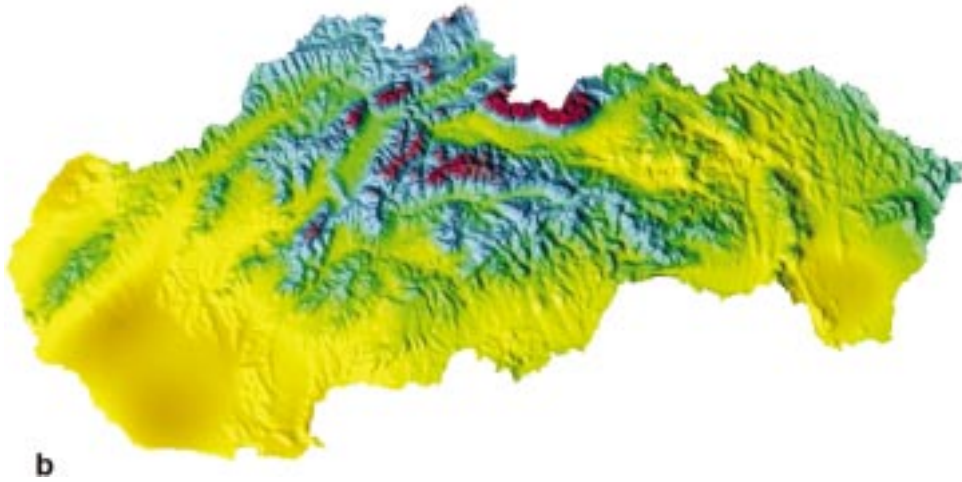
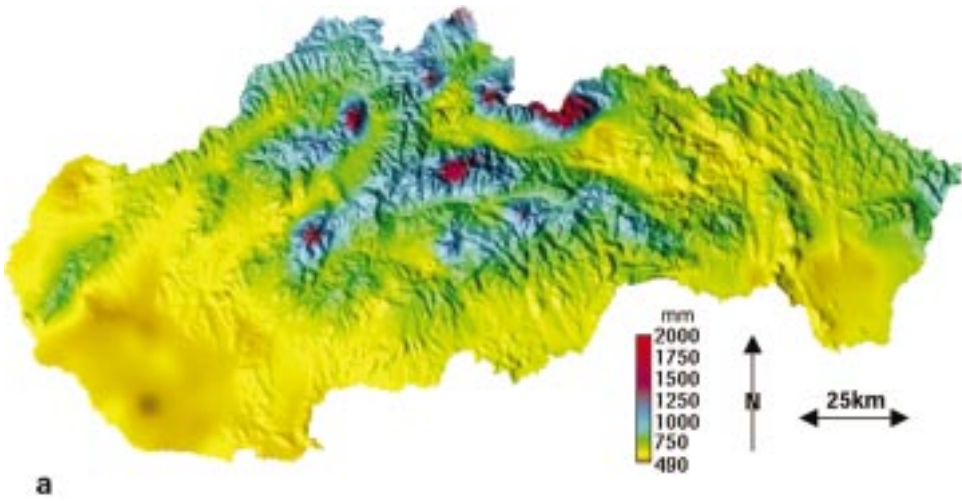


Plate 3 Annual mean precipitation maps for Slovakia interpolated by a) 2D RST, b) 3D RST

Plate 3 from J Hofierka, J Parajka, H Mitasova and L Mitas 'Multivariate Interpolation of Precipitation Using Regularized Spline with Tension', pages 135–150

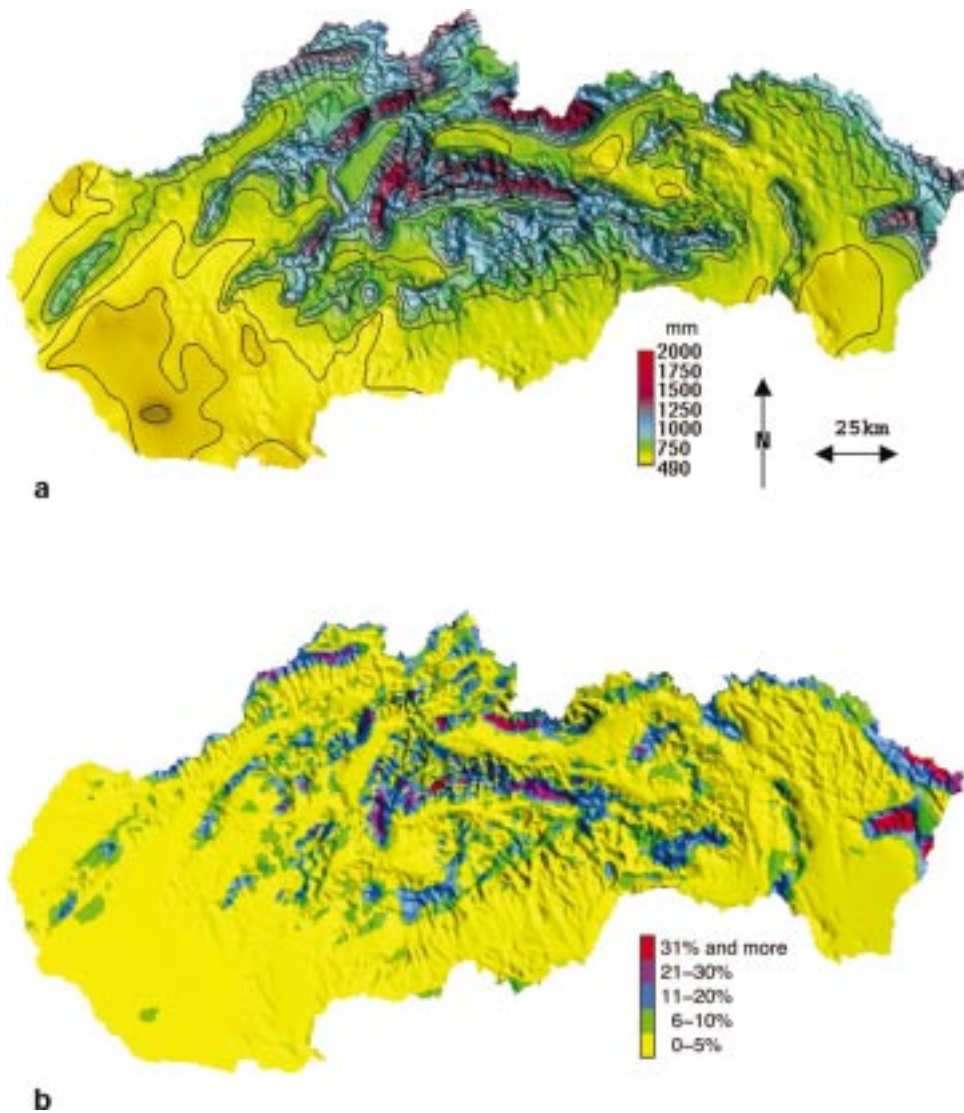


Plate 4 Evaluation of the 3D RST by comparison with a) expert-drawn precipitation map, b) absolute differences (in %) between the 3D RST precipitation map and expert-drawn precipitation map

Plate 4 from J Hofierka, J Parajka, H Mitasova and L Mitas 'Multivariate Interpolation of Precipitation Using Regularized Spline with Tension', pages 135–150

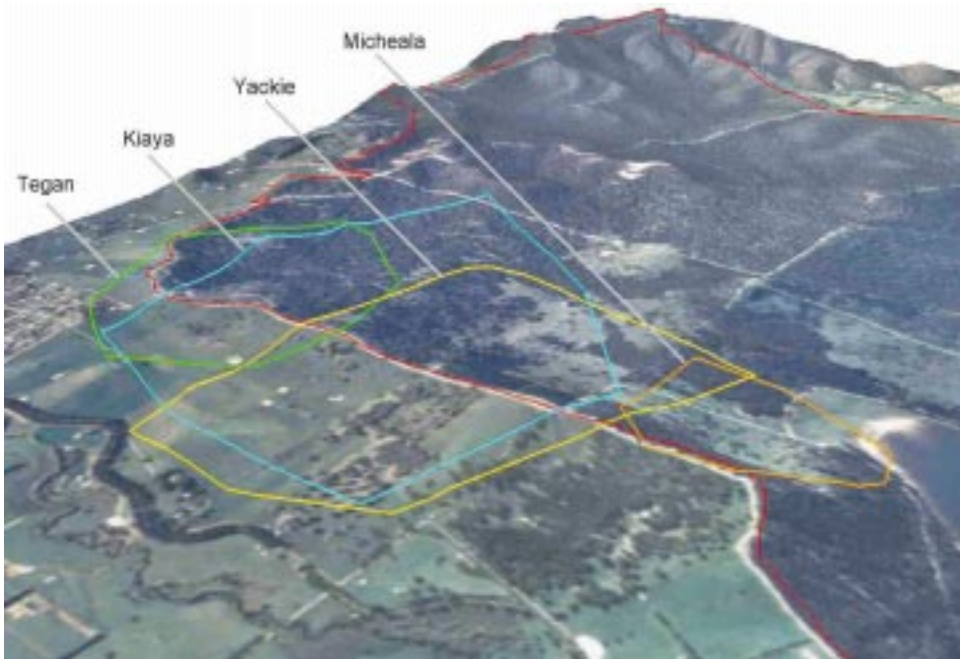


Plate 5 Perspective view of MCP HR estimates for the four kangaroos: Tegan (105.37 ha, Schoener index = 2.06), Kiaya (255.03 ha, Schoener index = 1.28), Yackie (166.76 ha, Schoener index = 2.08), and Micheala (35.41 ha, Schoener index = 1.74) from the southwest. HRs quoted as surface area. Colour greatly increases the quality of the image

Plate 5 from S W Selkirk and I D Bishop 'Improving and Extending Home Range and Habitat Analysis by Integration with a Geographic Information System', pages 151–159



Plate 6 Planar view of the $MAP_{FK(.95)}$ HR estimates for Tegan (thick line, 112.1 ha), Kiaya (speckled line, 239.9 ha), Yackie (thin line, 155.2 ha) and Micheala (dashed line, 43.7 ha). This image is easier to interpret when seen on the computer screen in colour. HR's as surface area

Plate 6 from S W Selkirk and I D Bishop 'Improving and Extending Home Range and Habitat Analysis by Integration with a Geographic Information System', pages 151–159



Plate 7 Time and season $MAP_{FK(.5)}$ Hr estimates for Tegan. Day HR = 27.4 ha (dashed line), night = 6.44 ha (full line), summer = 15.66 ha (dashed line), and winter = 12.71 ha (full line)

Plate 7 from S W Selkirk and I D Bishop 'Improving and Extending Home Range and Habitat Analysis by Integration with a Geographic Information System', pages 151–159



Plate 8 Observational data and the $MAP_{FK(.95)}$ HR estimate for Micheala. Catchment boundary fence (dashed line) from the RMDB is also shown

Plate 8 from S W Selkirk and I D Bishop 'Improving and Extending Home Range and Habitat Analysis by Integration with a Geographic Information System', pages 151–159